Available online at www.sciencedirect.com

ScienceDirect

Journal of Catalysis 255 (2008) 94–103

JOURNAL OF CATALYSIS

www.elsevier.com/locate/jcat

# Structural and reactive relevance of V + Nb coverage on alumina of V–Nb–O/$Al_2O_3$ catalytic systems

Anna E. Lewandowska [a,b], Miguel A. Bañares [a,*], Maria Ziolek [b], Dzhalil F. Khabibulin [c], Olga B. Lapina [c]

[a] Instituto de Catálisis y Petroleoquímica, CSIC, Marie Curie 2, E-28049 Madrid, Spain
[b] A. Mickiewicz University, Faculty of Chemistry, Grunwaldzka 6, 60-780 Poznan, Poland
[c] Boreskov Institute of Catalysis SB RAS, Prosp. Akad. Lavrentieva 5, 630090 Novosibirsk, Russia

Received 23 November 2007; revised 23 January 2008; accepted 23 January 2008

## Abstract

Vanadium and niobium species (together and separately) were loaded on gamma alumina, and the resulting catalysts were run in the methanol conversion. This reaction was studied by both GC analysis and FTIR study in the flow system. The catalytic properties are discussed based on the combined FTIR and $^{27}Al$, $^{51}V$ and $^{1}H$ MAS NMR studies. The NMR studies revealed a different mechanism of interaction between Nb and $Al_2O_3$ than that between V and $Al_2O_3$. This predetermines the structure of vanadium sites in bimetallic VNb/Al samples. The effect of coverage was considered for various metal loadings ranging from below to above monolayer. One of our most interesting findings is that the surface Nb oxide species exhibited a redox character below monolayer but were acidic above monolayer. $^{27}Al$ MAS NMR revealed a strong alumina–Nb interaction that may account for its redox performance. Moreover, the role of sulfate from vanadium precursor is evidenced.

*Keywords:* Supported vanadia–niobia; Alumina; $^{27}Al$ MAS NMR; $^{1}H$ MAS NMR; FTIR; *In situ*; Methanol probe reaction

## 1. Introduction

Vanadium- and niobium-containing catalysts are used in oxidation processes. In their supported forms, the support plays a critical role. If the oxide support exhibits its own activity in the desired reaction, then the loading level plays a crucial role in the final activity and selectivity of the prepared catalysts. In this work, various loadings of V and Nb on gamma alumina were applied, and the prepared catalysts were tested in methanol conversion.

Methanol oxidation has been proposed for the characterization of the redox and acidic active species on the catalyst surface. The structural information at the molecular level on the catalytic sites can be deduced from the product distribution in this reaction, e.g. [1–4]. Selective formation of dimethoxymethane ($(CH_3O)_2CH_2$) can be assigned to a dual site that includes a redox dehydrogenating site and a Lewis acid center, whereas formaldehyde ($CH_2O$) formation requires only a redox dehydrogenating site. Methyl formate ($HCOOCH_3$) can be generated *via* an oxidation reaction (redox centers), followed by dehydration (on acidic sites). The surface basic sites are responsible for CO + $CO_2$ formation. The selective formation of dimethyl ether ($CH_3OCH_3$) is assigned to the presence of strong acid sites.

Busca et al. [5] and Tatibouët [3] have provided very useful and informative schemes showing the reaction steps leading to the various products. These schemes allow differentiation of the oxidative and acidic routes of methanol oxidation and also aid identification of the intermediate chemisorbed species. Keep in mind, however, that the nature and adsorption strength of such chemisorbed species determine further reactions. Therefore, the estimation of chemisorbed species under real reaction conditions is very important to optimize the catalyst content. Taking this into account, we used an *in situ* flow reactor cell

---

[*] Corresponding author. Fax: +34 915854760.
*E-mail address:* banares@icp.csic.es (M.A. Bañares).

0021-9517/$ – see front matter © 2008 Elsevier Inc. All rights reserved.
doi:10.1016/j.jcat.2008.01.029

that allowed us to measure IR spectra under dynamic conditions.

We used multinuclear $^{27}$Al, $^{51}$V, and $^{1}$H solid-state NMR for structural characterization of alumina-supported vanadia, niobia, and vanadia–niobia catalysts. Today, $^{27}$Al and $^{51}$V solid-state NMR are indispensable to the study of many alumina- and vanadia-based catalysts and related materials. The coordination number of Al sites in AlOx can be readily determined from the value of the isotropic chemical shift [6,7]. $^{1}$H NMR of hydroxyl groups is very informative regarding the extent of dispersion of supported metal [8].

In this paper, we report on the preparation and characterization of structural and reactive properties of alumina-supported vanadia and niobia, and the effect of total V + Nb coverage on alumina.

## 2. Experimental

### 2.1. Preparation of samples

The vanadium and niobium oxides supported on alumina were prepared using different V precursors. The VS series was prepared using a $VOSO_4$ precursor, and the VM series was prepared using an ammonium metavanadate precursor. Vanadia on alumina catalysts were prepared from an aqueous solution of $VOSO_4$ (Aldrich, 99.99%), which was maintained under stirring at 323 K for 50 min, after which $\gamma$-$Al_2O_3$ (SASOL, $S_{BET} = 193\ m^2/g$) was added. The suspension thus obtained was evaporated in a rotatory evaporator at 338 K. The resulting solid was dried at 388 K for 20 h and then calcined at 673 K for 4 h in air. The rate of heating was 5 K/min. The impregnation of alumina-supported V–Nb and Nb oxides was done using $NH_4VO_3$ (Sigma, 99.99%) and $NH_4NbO(C_2O_4)_2$ (Aldrich, 99.99%) solutions. Oxalic acid (Panreac, 99.5%) was added to an aqueous solution of ammonium metavanadate and of ammonium niobate (V) oxalate to facilitate dissolution of salts. The same niobium precursor was applied in the preparation Nb/$\gamma$-$Al_2O_3$ system. Oxalic acid also was used for the impregnation of niobium on alumina. As a reference value, the monolayer value (understood to be the dispersion limit loading of the supported oxides) was estimated as a total number of 8 atoms (V + Nb)/nm$^2$ of alumina support. The amounts of V, Nb, and V + Nb were calculated so that the total coverage of metals ranged from ca. 1/4 of a monolayer to above monolayer. The V/Nb atomic ratio was kept at 1. The general $x$VS/Al (or $x$VM/Al), $x$Nb/Al and $x$VNb/Al nomenclature was applied, where $x$ indicates the number of atoms per nm$^2$ of V and Nb, S represents vanadyl sulfate, and M represents ammonium metavanadate.

### 2.2. NMR study

Solid-state NMR experiments were performed with Bruker AVANCE-400 (9.4 T) spectrometer at resonance frequencies 400.13, 104.26, and 105.20 MHz for $^{1}$H, $^{27}$Al, and $^{51}$V, respectively. A Bruker 4.0 mm, 2.5 mm MAS probes and NMR Rotor Consult ApS (Denmark) 5 mm MAS probe were used for static and 15- to 35-kHz MAS spectra acquisition. The single pulse sequence with rf-pulse length of 1 µs (12° flip angle) and recycle delay of 1–5 s was used to acquire $^{27}$Al and $^{51}$V spectra. $^{1}$H spectra were measured with pulse length of 10 µs (90°) and recycle delay of 1 s. The chemical shift values were referred to TMS for $^{1}$H, 0.1 M $Al(NO_3)_3$ for $^{27}$Al, and $VOCl_3$ for $^{51}$V.

$^{27}$Al 3QMAS (Triple-quantum MAS) experiments were performed using a basic 3-pulse sequence with z-filter. The sequence starts with an excitation pulse p1 (3.5 µs, corresponding to 180°) that creates 3Q coherence, which is allowed to evolve during the evolution period, $\tau$. A subsequent conversion pulse, p2 (1.0 µs, corresponding to 50°) flips magnetization back along the $z$-axis, which, after a short (20 µs) delay (to allow dephasing of undesired coherences), is read out with a weak CT-selective 90° pulse, p3 (6.5 µs).

The samples were dehydrated before the NMR experiments. The catalyst samples were placed into 7-mm glass ampules and dehydrated under vacuum ($<10^{-3}$ Torr) for 4 h at 623 K. Then they were calcined for 2 h at 723 K in dry $O_2$ and finally flame-sealed. Just before the measurements, the ampules were unsealed and the samples loaded into standard 5-mm rotors in a dry box under an argon flow. Hydration of the samples was achieved by exposing them to the humidity of the ambient air. $^{1}$H MAS NMR measurements were performed with dehydrated samples; $^{27}$Al NMR measurements, with hydrated ones. $^{51}$V MAS NMR was performed with both hydrated and dehydrated samples.

### 2.3. IR study

The IR experiments were performed with Vector 22 (Bruker) FTIR spectrometer. IR spectra were recorded at a resolution of 2 cm$^{-1}$ using 64 scans. The ~20 mg catalyst samples were pressed into thin wafers and placed in the *in situ* flow cell equipped with KRS-5 windows (insensitive to humidity). The activation, adsorption, and oxidation of methanol were carried out in this *in situ* flow cell. Spectra were registered in a temperature range of 373–573 K. The spectra without any sample ("gas phase") were scanned before each catalyst spectrum. Before the measurement, the samples were activated at 623 K in a 50 cm$^3$/min flow of oxygen and helium, which had been passed through a molecular sieve trap to remove moisture traces. The $O_2$/He molar ratio was 20/80. The pretreated materials (2 h) were gradually cooled to 373 K. Adsorption of methanol was performed at 373 K in a ~40 cm$^3$/min stream with a $CH_3OH$/He molar ratio 1.2/98.8. The methanol partial pressure was controlled by a methanol bubbler. IR spectra were recorded after 15 and 35 min of methanol adsorption. Methanol oxidation was carried out using gas mixture of $CH_3OH/O_2$/He (molar ratio 1.2/18.8/80) at a flow rate of ca. 40 cm$^3$/min. The temperature was gradually increased up to 573 K. IR spectra were obtained at given temperatures after 15 min of dwell time.

### 2.4. Methanol probe reaction

Methanol oxidation reaction was performed in a glass fixed-bed reactor equipped with a thermocouple. First, 0.03 g of cat-

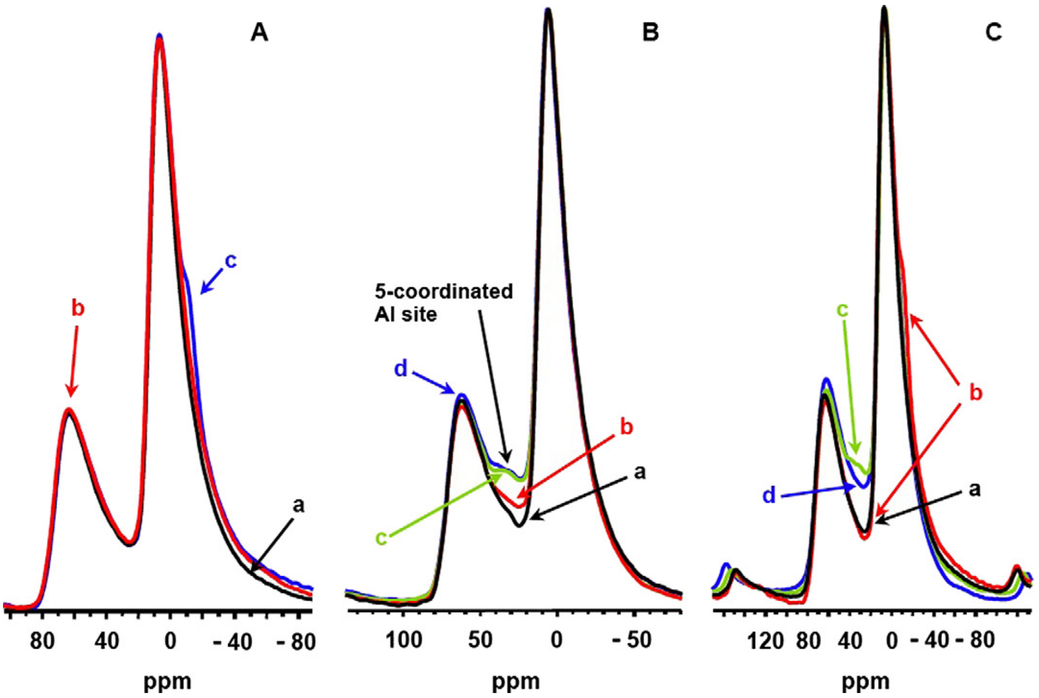

Fig. 1. $^{27}$Al MAS NMR spectra of: (A) V/Al catalysts: (a) 0.8VM/Al, (b) 2VS/Al, (c) 16VM/Al; (B) Nb/Al catalysts: (a) 4Nb/Al, (b) 6Nb/Al, (c) 8Nb/Al, (d) 16Nb/Al; (C) (a) $Al_2O_3$, (b) 16VM/Al, (c) 16Nb/Al, (d) 16VNb/Al. ($\nu_r = 10$ kHz.)

alyst was activated in a flow of air (40 $cm^3/min$) at 673 K. The oxidation reaction was carried out using a reaction feed of 40 $cm^3/min$ of $CH_3OH/O_2/He$ (molar ratio 1.5/15/83.5). The process was conducted at 408, 423, and 438 K. The catalyst was cleaned in an $O_2/He$ flow (flow rate $= 40$ $cm^3/min$) at 673 K for 30 min after every test, and then cooled to the specified temperature. Methanol and the reaction products were analyzed every hour with a SRI gas chromatograph with a flame ionization detector operated at a programmed temperature (308 K for 40 min, then heated at 10 K/min to 508 K).

## 3. Results and discussion

### 3.1. $^{27}$Al, $^{51}$V, and $^{1}$H MAS NMR

The interaction strengths between the matrix and supported oxides were estimated by $^{27}$Al MAS NMR. Pure $Al_2O_3$ exhibited two main NMR signals for the 6-coordinated Al site ($\delta^{27}$Al, 0 ppm) and the 4-coordinated Al site ($\delta^{27}$Al, 60 ppm). Fig. 1A shows the NMR spectra of the V/Al catalysts. $^{27}$Al MAS NMR for the vanadium catalysts prepared from different precursors (vanadyl sulfate and ammonium metavanadate) demonstrated no strong structural interactions between V and Al in V/Al. This feature appears to be mostly independent of vanadium loading. Only at very high vanadium content a new $^{27}$Al MAS NMR line appears at $-10$ ppm, corresponding to $AlVO_4$ species. The latter can be better seen in the corresponding 3Q MAS $^{27}$Al NMR spectrum (Fig. 2B) and also was confirmed by the $^{51}$V MAS spectrum (isotropic lines at $-668$, $-747$, and $-780$ ppm from $AlVO_4$) (Fig. 2A). Interaction of vanadia with alumina in V/Al materials also can be monitored by $^{1}$H MAS NMR of hydroxyl groups (Fig. 3), for which intensity versus loading is illustrated in Fig. 3A. Vanadium oxide species interacted with the surface of $Al_2O_3$ via bridged OH groups ($\delta^{1}$H, 1.6 ppm) and terminal OH groups ($\delta^{1}$H, $-0.2$ ppm), affecting the catalytic properties of the materials. Because both hydroxyl groups were almost depleted at monolayer coverage (8 atoms/$nm^2$), it makes sense to assume that vanadium oxide dispersion is directly linked to the availability of surface hydroxyl groups. At the same time, hydrogen-bonded hydroxyl groups ($\delta^{1}$H, 3.7 ppm) and bulk OH groups ($\delta^{1}$H 7.4 ppm) were much less affected. These data indicate high dispersion of surface vanadium oxide species over the support surface up to ca. 8 atoms/$nm^2$. There were no noticeable changes in the bulk $Al_2O_3$ structure. These findings indicate that the vanadia–alumina interaction is due mainly to surface reaction with alumina hydroxyl groups.

Whereas the V/Al catalysts did not demonstrate a strong interaction between the matrix and supported surface oxide species, the Nb/Al materials exhibited quite different behavior. $^{27}$Al MAS NMR spectra recorded for Nb/Al samples (Fig. 1B) show a characteristic $^{27}$Al resonance attributed to 5-coordinated Al sites [6]. The intensity of this line increased with increasing Nb content. It is reasonable to suggest stronger interactions of niobium with alumina, with possible incorporation of Nb into alumina. A different mechanism of interaction between Nb and $Al_2O_3$ compared with that between V and $Al_2O_3$ can be observed not only in the $^{27}$Al MAS NMR spectra, but also in the $^{1}$H MAS NMR spectra (Fig. 3B). Like the surface vanadia species, the supported niobia oxide species also interacted with the surface hydroxyl groups; however, at similar surface coverage values, the content of residual OH groups was always considerably higher in Nb/Al than in the V/Al series. This higher surface hydroxyl concentration may have had an effect on reactivity and suggests that the niobia species are not as widely

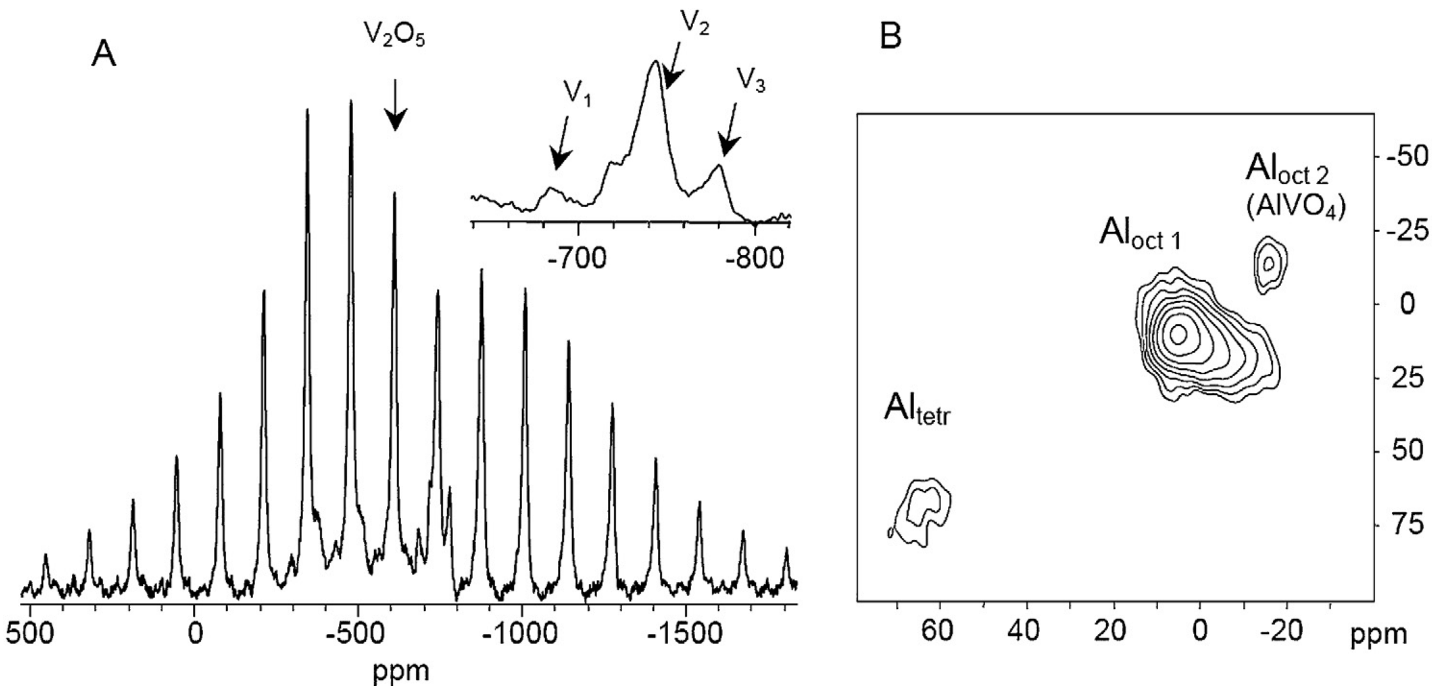

Fig. 2. (A) $^{51}$V MAS NMR, (B) $^{27}$Al 3QMAS NMR spectra of 16VM/Al catalyst. $^{51}$V MAS NMR spectrum is represented mainly by $V_2O_5$ (isotropic shift indicated in the spectrum) and small amount of surface species (lines in the bottom of the spectrum) and $AlVO_4$ insert in the right corner (isotropic lines from 3 nonequivalent vanadium sites are shown). Three sites from 4- and 6-coordinated Al are observed in $^{27}$Al 3Q MAS NMR spectrum.

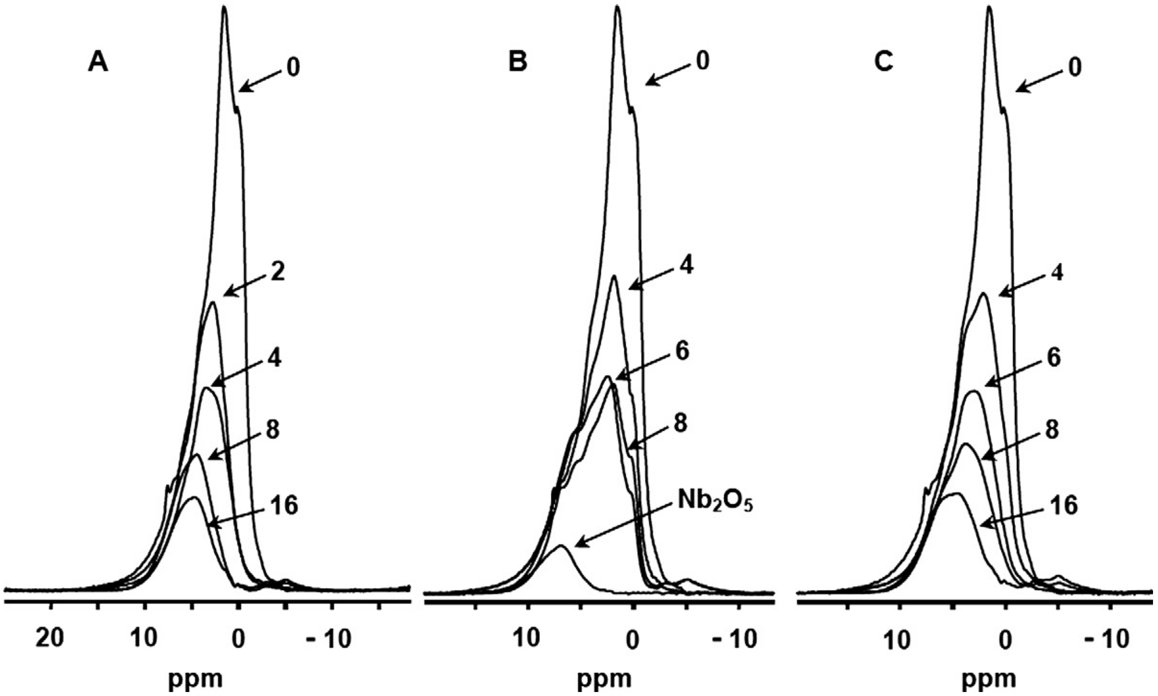

Fig. 3. $^{1}$H MAS NMR spectra of: (A) $x$VM/Al ($x = 0, 2, 4, 8, 16$), (B) $x$Nb/Al ($x = 0, 4, 6, 8$) and $Nb_2O_5$, (C) $x$VNb/Al ($x = 0, 4, 6, 8, 16$). ($\nu_r = 10$ kHz.)

dispersed as the vanadia species and thus tend to form more aggregates on the alumina surface. This island model of niobia deposition on the alumina surface appears very plausible. The $^{27}$Al MAS NMR results for VNb/Al are similar to those of Nb/Al, with no strong interactions between vanadia species and alumina support even at high Nb and V loadings (Fig. 1C). The $^{1}$H MAS NMR spectra evidence a monotonic decrease in the concentration of surface OH groups with mixed-metal oxide loading (Fig. 3C). All of these NMR findings can be understood from the island model scenario introduced above for the Nb/Al system: First, the niobia precursors interact strongly with the alumina surface, forming islands of mixed (Nb–Al) oxides, and

Table 1
Methanol oxidation flow bed reactor system at 438 K (GC analyses)

| | BET (m$^2$/g) | Methanol conversion (%) | Yield of products (%) | | | | Selectivity (%) | | | |
|---|---|---|---|---|---|---|---|---|---|---|
| | | | Dimethyl ether | Formaldehyde | Methyl formate | Dimethoxy methane | Dimethyl ether | Formaldehyde | Methyl formate | Dimethoxy methane |
| 4VM/Al | 178 | 46.2 | – | 43.5 | 2.7 | – | – | 93.5 | 6.5 | – |
| 4VS/Al | 175 | 29.6 | 2.5 | 26.2 | – | 0.9 | 8.6 | 88.4 | – | 3.0 |
| 6VS/Al | 142 | 27.7 | 1.3 | 25.2 | – | 1.2 | 4.9 | 91.0 | – | 4.1 |
| 8VS/Al | 117 | 39.0 | 1.9 | 33.3 | – | 3.8 | 5.0 | 85.4 | – | 9.6 |
| 4Nb/Al | 196 | 15.1 | 9.4 | – | 5.7 | – | 62.5 | – | 37.5 | – |
| 6Nb/Al | 140 | 28.1 | 3.8 | 19.6 | 4.2 | 0.5 | 13.6 | 70.0 | 14.7 | 1.7 |
| 8Nb/Al | 205 | 8.7 | 5.3 | – | 3.4 | – | 61.1 | – | 38.9 | – |
| 4VNb/Al | 182 | 15.1 | 7.4 | 5.0 | 2.1 | 0.6 | 48.6 | 33.9 | 13.7 | 3.8 |
| 6VNb/Al | 171 | 12.2 | 2.1 | 8.2 | 1.0 | 0.9 | 17.5 | 66.8 | 8.2 | 7.5 |
| 8VNb/Al | 172 | 22.4 | 1.6 | 19.8 | – | 1.0 | 7.5 | 88.2 | – | 4.3 |
| Al$_2$O$_3$ | 193 | 24.5 | 24.5 | – | – | – | 100 | – | – | – |

then the vanadia precursors interact with both Al$_2$O$_3$ and mixed (Nb–Al) oxide islands.

### 3.2. Methanol oxidation combined with GC analysis

Methanol oxidation in the flow system with GC analysis was carried out at relatively low temperature (438 K) to minimize side reactions. Table 1 summarizes the results. Alumina support produced DME only, characteristic of its surface acidic sites. Both V/Al materials demonstrated comparable interaction between surface vanadium species and the alumina surface, confirming the $^{27}$Al NMR findings (Fig. 1A). The differences between 4VM/Al and 4VS/Al underline the relevance of the precursor; DME formation was more evident for the VS series, which exhibited lower activity. The activity of catalysts VS/Al, Nb/Al, and VNb/Al depends on the transition metal loading. Vanadium-containing catalysts with the highest vanadium loading exhibited the highest methanol conversion; however, 4VS/Al and 6VS/Al showed similar activity profiles, accompanied by high selectivity to formaldehyde [9]. Taking into account the literature data, e.g. [1–3], the formation of formaldehyde in the methanol oxidation can be seen as an indicator of redox active centers. Thus, the results presented in Table 1 clearly indicate the dominant redox character of the vanadium-modified materials. This character was significantly enhanced when ammonium metavanadate (VM series) was used as vanadium source for the impregnation of alumina (4VM/Al sample); dimethyl ether is not detected by GC. Alumina-supported vanadia catalysts have greater polymerization degree compared with those prepared with VOSO$_4$, and surface polymerized vanadia is more reducible than isolated surface vanadia [10]. Surface sulfate species in VS/Al series must account for the acidic sites that yield DME. It is likely that the interaction between surface vanadia and sulfate species accounts for its lower polymerization degree.

The Nb/Al series exhibited a unique trend, which was confirmed by repeated experiments. Only 6Nb/Al catalyzed methanol to formaldehyde transformation; 4Nb/Al and 8Nb/Al produced DME and methylformate. All catalysts in the Nb/Al series have acidic and redox properties; formaldehyde is produced by redox sites, DME is produced by acidic sites, and methyl formate is produced *via* an oxidation reaction (redox centers), followed by dehydration (on acidic sites) [3,5]. However, the interplay among acidic and redox sites changes with changing niobia coverage. Interesting changes in performance were seen at niobia monolayer coverage (6 Nb atoms/nm$^2$); it exhibited the highest methanol conversion in the Nb/Al series and was essentially redox. Acidic sites were also seen to participate in the reactivity, affording DME and also methylformate; however, methylformate formation was significantly decreased. This indicates that acidic and redox sites were not immediate neighbors. The $^{27}$Al and $^{1}$H NMR studies revealed that surface niobium oxide species existed in islands that interacted strongly with alumina surface not only via OH groups, but also *via* additional bonds to Al. Monolayer coverage would lead to a minimum exposure of the niobia–alumina interface, which should have generated methylformate; in turn, it also would result in the maximum polymerization of niobia. The degree of polymerization is very important to oxidation processes on niobia catalysts [11,12]. At lower coverage, niobia species are less polymerized, which should decrease their redox properties. 4Nb/Al exhibited high selectivity to dimethyl ether (62.7%) as well as to methylformate (37.5%), with the former resulting from close interaction between redox niobia sites and their interface with alumina. In fact, the $^{27}$Al MAS NMR spectra showed an additional signal related to the 5-coordinated Al site formed through a strong interaction between niobium and aluminum species (Fig. 1B). At low coverage, alumina sites are exposed and exhibit acidic performance (selective to DME) [13,14]. At high niobia loading (8Nb/Al), bulky niobium oxide minimized the exposure of active sites, producing a scenario similar to that of the low coverage sample but with lower activity, as shown in Table 1.

The VNb/Al series exhibited an interesting trend of increasing conversion only for the sample with the highest loading. 4VNb/Al and 6VNb/Al had similar conversion values but very different selectivity trends. 4VNb/Al produced DME $>$ HCHO $>$ methylformate (48.6%, 33.9%, and 13.7% selectivity, respectively). DME is ascribed to acidic sites, similar to 4Nb/Al; however, the presence of surface vanadium oxide species produces formaldehyde and decreases the formation of methylformate. As V + Nb coverage increased, the system became

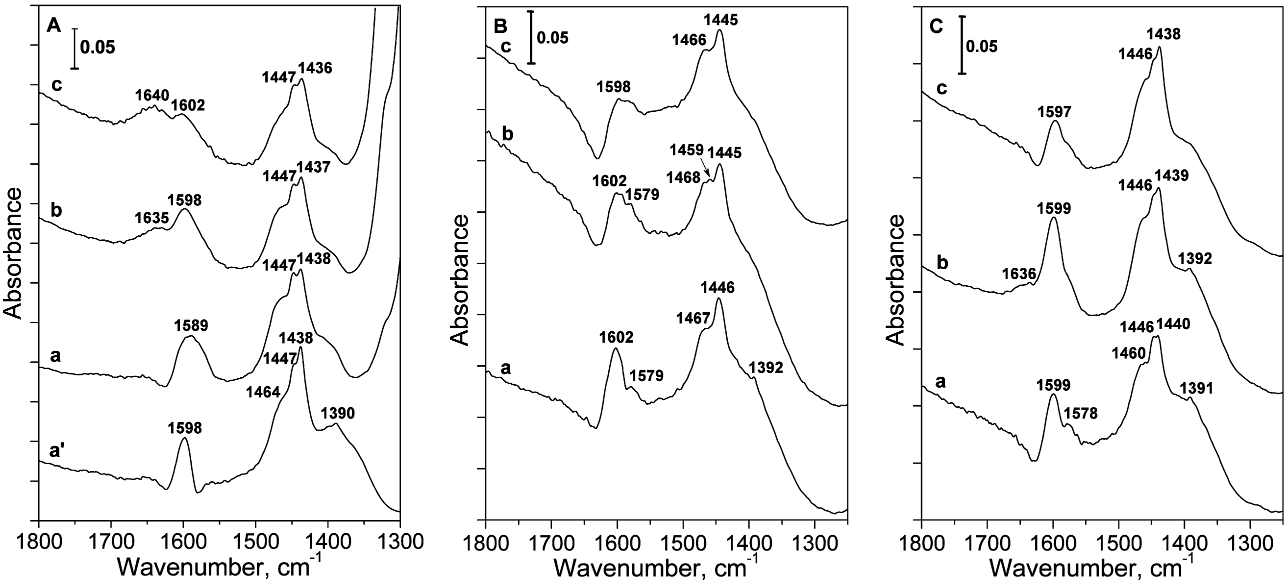

Fig. 4. FT-IR spectra of various metal (Me) loaded alumina after methanol adsorption at 373 K: (a) 4Me/Al, (b) 6Me/Al, (c) 8Me/Al, (a′) 4VM/Al; (A) VS/Al series; (B) Nb/Al series; (C) VNb/Al series.

less acidic and progressively more redox. 8NbV/Al produced no methylformate and much less DME; thus, only few acidic sites remained, and the interface between acidic and redox sites (methylformate) was no longer operative. This trend is consistent with a progressive coverage of niobia sites by vanadia, in concordance with $^{27}$Al MAS NMR data showing a very close Nb–Al interaction in which both Al and Nb sites combine in a mixed phase [15]. Therefore, vanadia dispersed on top of niobia-modified alumina. Selectivity trends on 8VNb/Al were very similar to those on alumina-supported vanadia catalysts.

Our findings for the VS/Al, Nb/Al, and VNb/Al catalysts reveal the paramount relevance of the interplay between acidic and redox sites for methanol conversion. Methanol transformation to methyl formate requires both redox and acidic centers; the presence of V and Nb accounts for both redox and acid sites, respectively. Dimethoxymethane also results from the oxidation of methanol, followed by the acid catalyzed intermolecular dehydration. Next, we discuss an *in situ* IR study of the species and active centers on the catalyst surface.

### 3.3. *FTIR study of methanol adsorption in flow system*

Before methanol oxidation, methanol was adsorbed on the catalyst surface at 373 K for 35 min. All FTIR spectra of the adsorbed methanol were obtained after equilibrium was reached for the methanol feed at the adsorbed phase. Fig. 4A shows the spectra of methanol adsorbed on the alumina-supported vanadium catalysts at the 1800–1300 $\text{cm}^{-1}$ IR range characteristic of $\delta$ vibrations. All spectra exhibited two sharp $\delta(\text{CH}_3)$ vibrational modes at 1447 and 1438 $\text{cm}^{-1}$, related to surface methoxy groups formed on the surface vanadium species [5,14,16]. The relative intensity of these two bands was almost independent of the vanadium loading but slightly dependent on the vanadium source used for impregnation. The poorly resolved band at around 1460 $\text{cm}^{-1}$ may be assigned to a methoxy group adsorbed on alumina [5,16]. This band was less pronounced in spectrum c, related to the adsorption on alumina with the highest vanadium oxide loading. The spectrum of 4VM/Al shows two more bands at 1390 and 1369 $\text{cm}^{-1}$ (Fig. 4Aa′). These bands [$\nu_\text{s}(\text{COO})$], along with the band at 1598 $\text{cm}^{-1}$ [$\nu_\text{as}(\text{COO})$], can be attributed to the surface formate species generated on the oxidizing centers [17]. Methyl formate was detected by GC in MeOH oxidation in the flow bed reactor but was absent in the released products in the reaction carried out on the other VS/Al, prepared from vanadyl sulfate. Formate species was detected in small amounts in spectra a–c in the materials prepared from vanadyl sulfate, suggesting a role of vanadium in the transformation of methoxy species toward formate. The increasing vanadium content in samples a–c led to an increased intensity of the band at $\sim$1640 $\text{cm}^{-1}$ (Fig. 4A, b and c). This may suggest the presence of water on the surface of the catalyst or may be assigned to $\nu(\text{CO})$ in chemisorbed formaldehyde. Water is formed in every route of methanol transformation. Formaldehyde was the main reaction product analyzed by GC. The formaldehyde species observed after methanol adsorption must result from the interaction between methoxy species and oxygen on the catalyst surface. Interestingly, bands due to the chemisorbed dimethyl ether were not seen, suggesting that the acidic route of methanol dehydration is not important under the used conditions.

The wavenumber range of 2700–3100 $\text{cm}^{-1}$ is less informative than the aforementioned one because of noise, which decreases the quality of spectra. Nevertheless, IR bands characteristic of methoxy species adsorbed on vanadium and alumina supports could be distinguished (Table 2): on vanadium, a $-2\delta_\text{s}(\text{CH}_3)$ band at 2827 $\text{cm}^{-1}$, a $\nu_\text{s}(\text{CH}_3)$ band at 2926 $\text{cm}^{-1}$, and a $\nu_\text{as}(\text{CH}_3)$ band at 2970 $\text{cm}^{-1}$; on alumina support, a $-2\delta_\text{s}(\text{CH}_3)$ band at 2842 $\text{cm}^{-1}$, a $\nu_\text{s}(\text{CH}_3)$ band at 2955 $\text{cm}^{-1}$, and a $\nu_\text{as}(\text{CH}_3)$ band at 2970 $\text{cm}^{-1}$ [1,5,14,16,18,19], especially on sample 4VM/Al. The VS/Al

Table 2
Observed wavenumbers of the $CH_3$ stretching modes of the methoxy groups after methanol adsorption at 373 K

| Assign. | Methoxy groups ($cm^{-1}$) | | | | | | | | | | | | |
|---|---|---|---|---|---|---|---|---|---|---|---|---|---|
| | 4VM/Al | 4VS/Al | 6VS/Al | 8VS/Al | $Al_2O_3$ | 4Nb/Al | 6Nb/Al | 8Nb/Al | $Al_2O_3$ | 4VNb/Al | 6VNb/Al | 8VNb/Al | $Al_2O_3$ |
| $\nu_{as}(CH_3)$ | 2970 | 2960 | 2958 | 2960 | 2970 | 2959 | | 2964 | 2968 | 2963 | 2957 | 2959 | 2969 |
| $\nu_s(CH_3)$[a] | 2926 | 2929 | 2929 | 2931 | 2955 | 2940 | 2946 | 2938 | | 2939; 2926 | 2935; 2929 | 2939; 2927 | 2950 |
| $2\delta_s(CH_3)$[a] | 2827 | 2828 | 2830 | 2830 | 2842 | 2828 | 2825 | 2830 | 2845 | 2830 | 2830 | 2832 | 2842 |
| $\nu_{as}(CH_3)$[b] | | 2955 | 2958 | 2951 | | | | | | | | | |
| $\nu_s(CH_3)$[b] | | 2851 | 2849 | 2847 | | | | | | | | | |

[a] Fermi resonances.
[b] Associatively chemisorbed $CH_3OH$.

series, prepared from vanadyl sulfate, also exhibited bands at ca. 2850 and 2955 $cm^{-1}$ (Table 2), which may be assigned to associatively chemisorbed $CH_3OH$ [20]. Vanadium oxide loading decreased the relative intensity of the bands of $CH_3O$ groups on alumina and of associatively adsorbed methanol.

Spectra of the adsorbed species formed during methanol adsorption on niobium supported alumina are presented in Fig. 4B. Two sharp $\nu(CH_3)$ bands at 2959 and 2940 $cm^{-1}$, a $2\delta_s(CH_3)$ band originating from Fermi resonance at 2828 $cm^{-1}$ (Table 2), and $\delta(CH_3)$ vibrational modes at 1446 $cm^{-1}$ were observed for the 4Nb/Al catalyst (Fig. 4Ba). These bands are related to surface methoxy group adsorbed on niobium. Bands at 2968, 2845, and 1467 $cm^{-1}$ can be attributed to surface methoxy groups adsorbed on $Al_2O_3$. Two bands at ~1600 and 1392 $cm^{-1}$ visible in the FTIR spectrum of 4Nb/Al can be assigned to formate species [5,16,17,19]. At higher Nb coverage, these bands were less resolved. Two shoulders at 1478 and 1459 $cm^{-1}$ were observed on the 6Nb/Al sample (Fig. 4Bb), attributed to dimethyl ether chemisorbed on the surface. This corresponds to the lowest selectivity to dimethyl ether in this sample detected by GC in the flow bed reactor system. Overly strong chemisorption of either species will decrease its desorption to the gas phase. This suggests a stronger acidic character of niobium species compared with vanadium species. The FTIR band at 2916 $cm^{-1}$ and shoulder at 2821 $cm^{-1}$ likely can be attributed to methoxy groups originating from the methyl formate adsorbed on niobia [11].

FTIR spectra of methanol adsorbed on mixed VNb/Al materials are shown in Fig. 4C. The introduction of two species (V and Nb) on the alumina surface enriched the IR spectra of these catalysts. The $\nu(CH_3)$ bands at 2968, 2963, 2950, 2939, and 2926 $cm^{-1}$, two $2\delta_s(CH_3)$ bands at 2842 and 2830 $cm^{-1}$, and $\delta(CH_3)$ vibrational modes at 1467, 1460, 1446, and 1440 $cm^{-1}$ appeared during methanol adsorption. These can be assigned to methoxy groups adsorbed on the vanadium and niobium surface species, as well as on $Al_2O_3$. V and Nb coverage decreased the bands related to methoxy species adsorbed on alumina (2950, 2842, and 1460 $cm^{-1}$) [16,18]. An insignificant amount of associatively chemisorbed $CH_3OH$ was also observed on the 6VNb/Al material (Fig. 4Cb). The 4VNb/Al catalyst, similar to the 4VM/Al and 4Nb/Al catalysts, exhibited IR bands due to the formate species [21]. Vanadium and niobium loading decreased these bands at 1578, 1391, and 1370 $cm^{-1}$. A weak shoulder at 1288 $cm^{-1}$ may be assigned to dimethyl ether species.

Among the materials studied in the present work, only alumina modified by vanadyl sulfate demonstrated methanol adsorption in the associatively chemisorbed form. This finding suggests that the type of the vanadium precursor used in the preparation of materials affects the type of the adsorbed species, which of course determines the further transformation of reagents. Of note, the presence of sulfate ions on the VS/Al catalysts was demonstrated by the intense absorption below 1300 $cm^{-1}$ (Fig. 4A).

### *3.4. Methanol oxidation in the flow system combined with FTIR study*

Figs. 5A–5D illustrate the effect of methanol oxidation at various temperatures on 4Me/Al samples. On the FTIR spectra in the 1300–1800 $cm^{-1}$ region are shown. It is noteworthy that during the methanol oxidation process, all catalysts exhibited dimethyl ether in the gas phase detected in IR gas-phase spectra. This finding is in line with the foregoing results of the experiments in the flow bed reactor and GC analysis on all but the 4VM/Al catalyst (Table 1). The amount of the produced ether depends on the composition of the catalyst. The FTIR spectra of 4VS/Al during $CH_3OH$ oxidation, presented in Fig. 5A, show that the intensity of the bands related to the methoxy groups adsorbed on vanadium (1448 and 1437 $cm^{-1}$) and on alumina (1464 $cm^{-1}$) decreased with reaction temperature. This effect was significant above 523 K. The shoulders at 1474 and 1464 $cm^{-1}$ can be attributed to traces of dimethyl ether chemisorbed on the surface (the latter overlapping with that from methoxy species on alumina). The new bands at 1479, 1408, and 1393 $cm^{-1}$ became well visible at the elevated temperature (Fig. 5Ae); these may be assigned to polyoxymethylene species (and possibly also dioxomethylene)–$CH_2$ bending vibrations [11,17,19]. This finding suggests the polymerization of formaldehyde adsorbed on the catalyst surface [11]. This effect was not so evident on the samples with higher vanadium oxide loadings. The polymerization process requires OH or basic sites [17]; the OH sites can be generated by the sulfur species located on the surface, especially when traces of moisture are present [17,22,23]. The aforementioned band at 1393 $cm^{-1}$ overlaps with bands from chemisorbed formate species $\nu_s(COO)$ and $\nu_{as}(COO)$ at ~1390 and ~1600 $cm^{-1}$ [17].

Regarding formaldehyde polymerization, the difference between the 4VS/Al and 4VM/Al catalysts is shown in Fig. 5. The

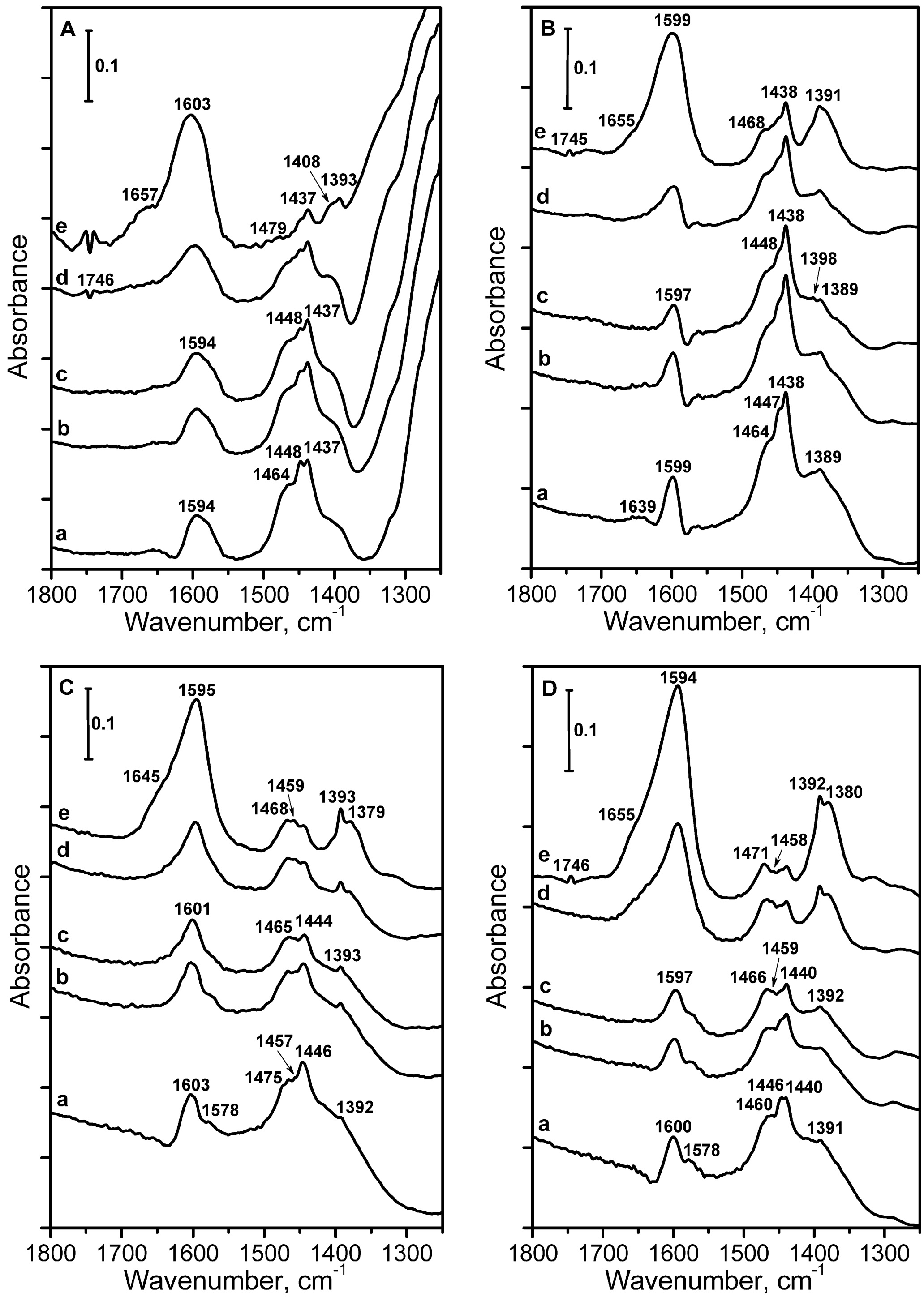

Fig. 5. FT-IR spectra during methanol oxidation at: (a) 373, (b) 423, (c) 473, (d) 523, and (e) 573 K of (A) 4VS/Al; (B) 4VM/Al; (C) 4Nb/Al; (D) 4VNb/Al.

latter was not active in this side reaction route. This leads us to the conclusion that the sulfate ions, strongly held on the catalyst surface even at 573 K (absorption below 1300 $\text{cm}^{-1}$), may be involved in this polymerization process.

Comparing the IR spectra of chemisorbed methanol (Fig. 5A) and *in situ* during methanol reaction (Fig. 5B) underscores an interesting difference: more intense formate species bands (1398 and 1389 $\text{cm}^{-1}$) and less intense bands of chemisorbed formaldehyde ($\sim$1650 $\text{cm}^{-1}$) on 4VM/Al than on 4VS/Al. More weakly bound formaldehyde desorbs more readily, and the free active centers are available for additional methanol chemisorption. This makes the catalyst more active, as evidenced from the results reported in Table 1.

Methyl formate genesis requires the concurrence of two kinds of active centers at the catalyst surface (acidic and redox), in line with the reaction pathway proposed by Busca et al. [5]. The lower intensity of IR band from methyl formate on the VS/Al materials may suggest that sulfate species poisons

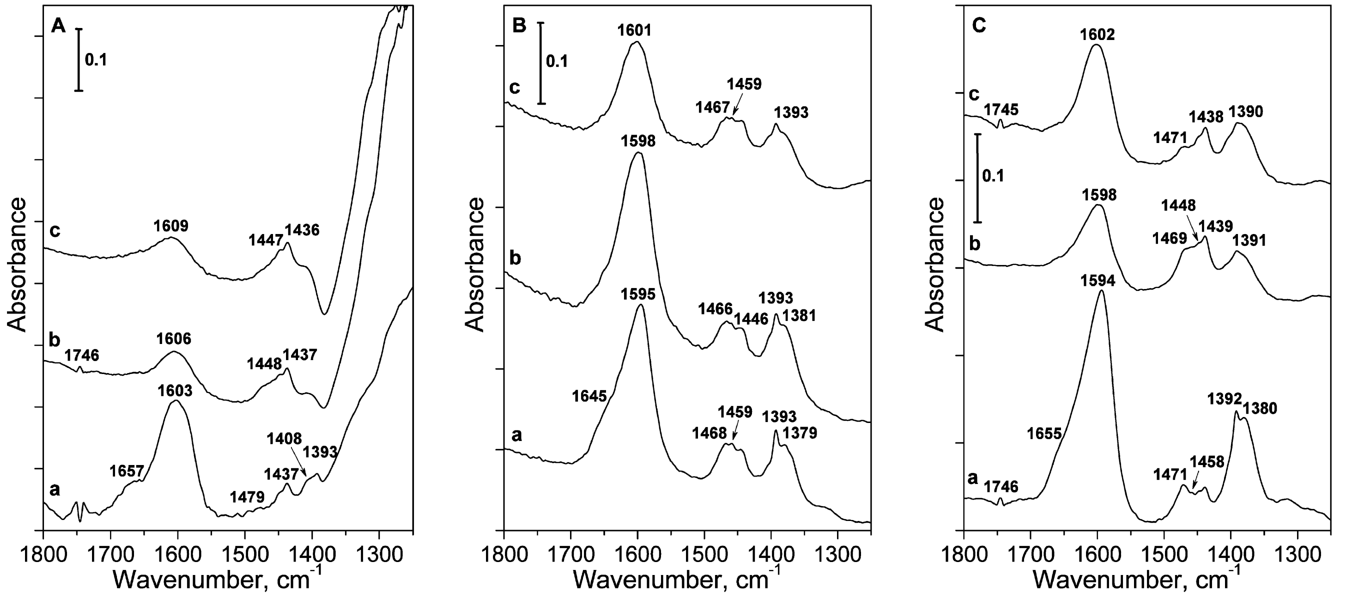

Fig. 6. FT-IR spectra of various metal (Me) loaded alumina during the methanol oxidation at 573 K: (a) 4Me/Al, (b) 6Me/Al, (c) 8Me/Al; (A) VS/Al series; (B) Nb/Al series; (C) VNb/Al series.

the second active site, likely an oxygen site on the alumina surface or an oxygen trap. This phenomenon may be responsible for the nondissociated methanol adsorption on the VS/Al catalysts, which was not seen on the other materials studied.

The spectra of alumina-supported niobium oxide (4Nb/Al) during methanol reaction were dominated by two chemisorbed species: dimethyl ether and methyl formate (Fig. 5C). The bands at ~1600 and 1392 $\text{cm}^{-1}$ can be assigned to formate species; the bands at 1475 and 1457 $\text{cm}^{-1}$, to dimethyl ether. Both species were present on the surface of 4Nb/Al catalyst even at 373 K (Fig. 5Ca), and both were the main reaction products in the GC analyses described above (Table 1). The oxidation products coexisted on the surface with methoxy groups adsorbed on niobium; however, the bands of the methoxy species diminished with reaction temperature. The intensity of the bands of chemisorbed formate (at 1595, 1393, and 1379 $\text{cm}^{-1}$) increased with the reaction temperature (Fig. 5Ce). The intensity of the bands of chemisorbed ether demonstrated no significant changes, however. On the other hand, the presence of dimethyl ether in the gas phase, as confirmed by online FTIR analysis of the gas phase and by GC analyses (Table 1), suggests that ether was not strongly chemisorbed on the catalyst surface.

FTIR spectra of 4VNb/Al during $CH_3OH$ oxidation, shown in Fig. 5D, clearly reveal adsorption of formate species on the catalyst surface (bands at 1594, 1392, and 1380 $\text{cm}^{-1}$) even at low reaction temperatures, increasing significantly with reaction temperature. Simultaneously, the bands related to methoxy groups were considerably diminished. These FTIR spectra also show traces of the formaldehyde (1746 $\text{cm}^{-1}$) in the gas phase and ether species (1471, 1458 $\text{cm}^{-1}$) on the catalyst surface at the highest temperature (Fig. 5De).

The 4VNb/Al catalyst exhibited the most intense bands of formate species among all of the catalysts shown in Fig. 5. This indicates easy formation of this product (note that it requires the presence of two sites) on the one hand, and relatively strong chemisorption on the other hand.

The other important consideration in the present work is the effect of metal loading on alumina. The results obtained at 573 K are shown in Figs. 6A–6C. Interestingly, the intensities of IR bands due to the chemisorbed formate species (at ~1380, ~1390, and ~1600 $\text{cm}^{-1}$) were the highest for the lowest metal loadings in all three series of catalysts. As mentioned earlier, based on the proposal of Busca et al. [5], the generation of formate species involves not only the supported oxide site, but also oxygen from the catalyst surface. The highest intensity of the IR bands due to formate on the 4Me/Al samples demonstrates the participation of alumina oxygen or alumina oxygen trap (i.e., the interface between the supported phase and alumina) in this reaction step. This accounts for the relevance of alumina coverage. Along this line, the effect of sulfate ions would be to block alumina active species on the VS/Al series; this is consistent with the absence of methyl formate species on VS/Al catalysts (Table 1).

## 4. Conclusions

Based on our findings, we can state the following conclusions:

1. Our $^{27}$Al, $^{51}$V, and $^{1}$H MAS NMR studies revealed different mechanisms of interaction between supported surface oxide species and the alumina surface. Highly dispersed surface vanadia species bound to $Al_2O_3$ surface via bridged and terminal OH groups were shown in V/Al systems. A strong interaction between Nb and Al, with possible incorporation of Nb into alumina detected in Nb/Al samples, is described by the island model of niobia deposition on the alumina surface. The island model also describes the bimetallic (VNb/Al) catalysts. In this case, the niobia pre-

cursors interact strongly with the alumina surface, forming islands of mixed (NbAl) oxides; then vanadia precursors interact with both oxides and disperse randomly on the surfaces of $Al_2O_3$ and mixed (NbAl) oxide islands.

2. Vanadium-containing materials are highly active for the oxidation of methanol toward formaldehyde. The use of vanadium sulfate as V source diminishes the total activity, but also decreases the formation of formate species by blocking alumina sites.
3. The generation of formate species requires the presence of oxygen sites from the alumina support and from the supported oxide phase.
4. Niobium-containing materials catalyze mainly an acidic route in the methanol probe reaction, resulting in production of dimethyl ether and the combined redox–acidic reaction product (methylformate). However, it is possible to find such a niobium loading (in this study, 6Nb/Al) that gives rise to the typical redox activity toward formaldehyde formation. This reflects the critical nature of the interplay between acidic and redox sites in conditions in which both are readily available to reactants.
5. The bimetallic catalyst series (VNb/Al) shifts from acid–redox to increasingly redox with increasing V + Nb oxide loading. The activity and reaction *in situ* FTIR trends are consistent with vanadium oxide species covering niobium sites.

## Acknowledgments

This work was supported by NATO grant ESP.NR. NRCLG 981857, Spanish Ministry of Education and Science project CTQ2005-02802/PPQ, RFBR grant 07-03-00695-a, COST action D36, WG No D36/0006/06, and Polish Ministry of Science grant 118/COS/2007/03. A.E.L. thanks the Spanish Ministry of Education and Science for a "Juan de la Cierva" postdoctoral fellowship.

## References

[1] J.-M. Jehng, A.M. Turek, I.E. Wachs, Appl. Catal. A 83 (1992) 179.
[2] X. Gao, I.E. Wachs, M.S. Wong, J.Y. Ying, J. Catal. 203 (2001) 18.
[3] J.M. Tatibouët, Appl. Catal. A Gen. 148 (1997) 213.
[4] M. Trejda, J. Kujawa, M. Ziolek, Catal. Lett. 108 (2006) 141.
[5] G. Busca, A.S. Elmi, P. Forzatti, J. Phys. Chem. 91 (1987) 5263.
[6] J. Klinowski, Prog. Nucl. Magn. Reson. Spectrosc. 16 (1984) 237.
[7] K.J.D. MacKenzie, M.E. Smith, Multinuclear Solid State NMR of Inorganic Materials, Pergamon/Elsevier, Oxford, 2002.
[8] V.M. Mastikhin, I.L. Mudrakovsky, A.V. Nosov, Prog. Nucl. Magn. Reson. Spectrosc. 23 (1991) 259.
[9] F. Roozeboom, P.D. Cordingley, P.J. Gellings, J. Catal. 68 (1981) 464.
[10] M.V. Martínez-Huerta, X. Gao, H. Tian, I.E. Wachs, J.L.G. Fierro, M.A. Bañares, Catal. Today 118 (2006) 279.
[11] G.J. Millar, C.H. Rochester, K.C. Waugh, J. Chem. Soc. Faraday Trans. 87 (1991) 2785.
[12] M. Ziolek, Catal. Today 78 (2003) 47.
[13] R.S. Schiffino, R.P. Merrill, J. Phys. Chem. 97 (1993) 6425.
[14] L.J. Burcham, I.E. Wachs, Catal. Today 49 (1999) 467.
[15] A.E. Lewandowska, O. Lapina, M. Ziolek, D.F. Khabilulin, M.A. Bañares, XXXI Bienal Conference of RSEQ, Book of abstracts. Toledo, Spain (2007) 147.
[16] G. Busca, Catal. Today 27 (1996) 457.
[17] G. Busca, J. Lamotte, J.-C. Lavalley, V. Lorenzelli, J. Am. Chem. Soc. 109 (1987) 5197.
[18] G. Busca, P.F. Rossi, V. Lorenzelli, M. Benaissa, J. Travert, J.-C. Lavalley, J. Phys. Chem. 89 (1985) 5433.
[19] G. Busca, J. Mol. Catal. 50 (1989) 241.
[20] A. Senallach, R. Meyer, H.H. Gunthard, J. Mol. Spectrosc. 52 (1974) 94.
[21] G.J. Millar, C.H. Rochester, K.C. Waugh, J. Chem. Soc. Faraday Trans. 87 (1991) 2795.
[22] O. Saur, M. Bensitel, A.B. Mohammed Saad, J.-C. Lavalley, C.P. Tripp, B.A. Morrow, J. Catal. 99 (1986) 104.
[23] M. Waqif, J. Bachelier, O. Saur, J.-C. Lavalley, J. Mol. Catal. 72 (1992) 127.